Delft University of Technology
Master's Thesis in Embedded Systems

Enabling Location-based Services using Wearable and Handheld

Luis Henrik John

embedded software

TU Delft Delft University of Technology

Enabling Location-based Services using Wearable and Handheld

Master's Thesis in Embedded Systems

Embedded Software Group
Faculty of Electrical Engineering, Mathematics and Computer Science
Delft University of Technology
Mekelweg 4, 2628 CD Delft, The Netherlands

Luis Henrik John
l.h.john@student.tudelft.nl

17th October 2016

Author
Luis Henrik John (l.h.john@student.tudelft.nl)
Title
Enabling Location-based Services using Wearable and Handheld
MSc presentation
28th October 2016

Graduation Committee

Prof. dr. K.G. Langendoen (chair)	Delft University of Technology
Dr. R. Venkatesha Prasad	Delft University of Technology
Dr. A. Bozzon	Delft University of Technology
MSc. Chayan Sakar	Delft University of Technology

Abstract

Smartphones, or more general handhelds, which are commonly used for indoor localization purposes, are not a viable option in places where people do not carry them all the time, e.g., home and office. Alternatively using wearable devices brings along limitations in regards to power supply, processing capability and availability of sensors, which prevents the adoption of many common handheld localization solutions. In this work a distributed localization system is presented, using wearable and handheld jointly, to address these drawbacks. Using only a magnetometer, an accelerometer, and Bluetooth radio, localization is performed by means of a particle filter. In addition, a smart handoff mechanism is presented, which uses the wearable only when it is necessary, thus reduces energy consumption on the wearable without affecting the desired location accuracy. Evaluating the system with ten participants, a localization accuracy of 90.31 % in an indoor environment spanning about 320 m^2 was achieved.

Preface

The motivation for the research topic arose from the need of a pervasive localization system when offering contextual location-based services in non-public indoor environments. This report should show the necessity for wearable localization and provide an infrastructure approach for future intelligent service provisioning.

Luis Henrik John is a MSc student in Embedded Systems at Delft University of Technology.

Delft, The Netherlands
17th October 2016

Contents

List of Figures

List of Tables

List of Algorithms

Chapter 1

Introduction

As people spend approximately 90 % of their time in indoor environments [1], personal indoor localization has been considered an important constituent of pervasive computing applications [2]. Lymberopoulos *et al.* [3] broadly categorize indoor localization techniques into two classes – (i) infrastructure-based, and (ii) infrastructure-free. Since the former often involves expensive deployments in regards to time and money, it renders less suitable for most such applications. Thus, in the notion of pervasive computing, infrastructure-independence is usually favorable.

Existing indoor localization systems generally localize an embedded system, which in turn localizes the user. A pervasive interface device commonly utilized for this purpose is the handheld [4, 5, 6], as it offers a variety of sensors and large processing capability. Such solutions make the user invariably device dependent, which is appropriate for most public indoor spaces such as shopping malls or airports. However, they are less applicable for home and office environments, where users may not carry such a device all the time; handhelds are left behind on desks, tables, or sofas, and remain static for long durations. Users within such non-public indoor spaces should represent the target audience of this work.

Recently, wearable devices – holding energy efficient sensing and computing modules – have become increasingly available [7]. They range from smartwatches, over fitness trackers, body-worn cameras, to head-mounted displays and smart garment. Even though the processing capabilities of these devices are often lower compared to handhelds, they are able to track and measure various human activities continuously, as they are envisioned to be worn on the body all the time. This provides the opportunity to utilize wearable devices for ubiquitous indoor localization.

1.1 Use cases

Location-based service provisioning in non-public indoor spaces, such as home and office, is diverse. Various monitoring, control, and contextual services can be optimized by accurate localization techniques. For example, Sarkar *et al.* [8] proposed a room-level indoor lighting and heating control system that relies on locations of the occupants to provide a comfortable living and working environment. Apart from this, elderly care systems can utilize location information of a person to track activities remotely and cross reference them with the location to acquire better accuracy [9]. Applications for fall detection could enable healthcare personal to track the location of a user more precisely and prepare appropriate support [10]. Intelligent systems, such as personal assistant responsible for time and task management could be enriched by location information to provide more dynamic range of features for the user, such as rescheduling meetings when a person has not left the bedroom and is expected to have overslept [11]. All such applications along with any future use-cases will benefit from wearable-based localization systems.

1.2 Challenges

To achieve a small form factor, most wearables have limited battery size, lower processing power, and a smaller number of sensors as compared to their handheld counterparts. Of all the wearables, currently, only smartwatches can offer comparable processing capabilities and sensors as handhelds. However, out of 274 M wearable devices that are projected to be sold worldwide in 2016, only about 18 % are smartwatches [7]. On an average, smartphones sold in 2016 have a battery capacity of 2516 mAh, ranging from 650 mAh up to 5000 mAh [12]. Tablets, due to larger size, can even provide larger capacities. On the other hand, smartwatches are ranging from 200 mAh to 400 mAh [13], which is the reason for more efficient, and hence, less capable processing units. Thus, handheld-based indoor localization solutions cannot be easily adapted for most of the affordable and less complex wearables. For these reasons, a distributed localization system using wearable and handheld is envisioned. The wearable guarantees completeness of sampled sensor data, while the handheld, even if not collocated with the user anymore, can be responsible for demanding processing tasks. To do so a number of challenges need to be tackled.

- The radio communication between handheld and wearable, and sensor sampling frequencies need to be limited. As continuous sampling of not required sensors is inefficient from an energy point of view, it has to start and stop in an optimized way.

- Integrating only a limited number of sensors in commercial wearables is a consequence of a smaller form factor and battery capacity. The lack of sensors or radio interfaces can limit the use of traditional infrastructure-free and infrastructure-based localization methods [6, 14, 15, 16].

- Devices and their components are developed by various manufacturers. The feasibility of a wearable needs to be confirmed by a prototype using common electronic components.

1.3 Contributions

A localization system jointly using wearable and handheld for non-public indoor spaces is proposed. The assumptions are that the wearable is of low complexity, holding only an integrated accelerometer and magnetometer, and can be connected with the handheld using a Bluetooth radio. Considering a lack of infrastructure in the indoor environment, the wearable will be localized relative to the handheld's absolute location, which is assumed to be acquired by one of the common handheld-based localization techniques [17, 4, 5, 6].

Wearable functions include step detection, heading estimation and deduction of distance between the two devices. When localization switches between handheld and wearable a dynamic handoff takes place to avoid sampling sensors of both devices continuously. The challenges are approached by employing a particle filter computed on the handheld, merging information received from the wearable on a floor plan. Computing approximations to posterior distributions causes particle convergence due to map constraints, which again indicates location of the wearable by eliminating location ambiguity. The specific contributions of this work are as follows.

- A practical localization solution for location-based pervasive services is presented. The joint localization system uses a pair of wearable and handheld.

- To overcome the processing limitations of a wearable, computational tasks are delegated to a handheld without incurring significant energy consumption.

- A dynamic handoff mechanism ensures that not required sensors on both devices are switched off whenever possible.

- This non-intrusive, infrastructure-free, and pervasive localization system provides room-level accuracy. Based on an evaluation with ten participants, on an area of about $320\,\mathrm{m}^2$ comprising of 10 rooms, an accuracy of 90.31 % is achieved.

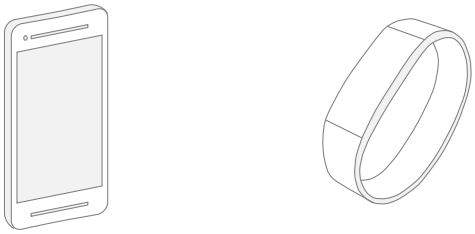

Figure 1.1: Common commercially available handheld smartphone and wearable fitness wristband.

1.4 System summary

The generic terms handheld and wearable will be used throughout this report to describe the involved embedded devices for the localization system (Fig. 1.1). A handheld is an interface device, commonly held in the hand when operated and otherwise resting in pockets or bags close to the body, unless left behind on furnitures. Examples for handheld devices are smartphones, but also tablets and e-book readers. On the contrary, a wearable is worn on the body, mostly with direct skin contact and thus can be assumed to be with the user throughout the day, that can even include activities such as sleeping or taking a shower. Wearables are available as smartwatches, head-mounted displays, body-worn cameras, bluetooth headset, wristbands, smart garments, chest straps and other fitness monitors.

Fig 1.2 gives a scenario for the proposed system operation. A floor plan is presented of an indoor environment. Considering the following scenario, the benefits of wearable localization become apparent. A user arrives via the staircase (room 1) at her home. She is carrying her handheld device, which she drops off in the living room (room 2). Shortly after, she proceeds to the kitchen (room 8) to prepare dinner, and after that, transfers to the dining room (room 3). In this time, handheld localization is interrupted and wearable localization needs to be active, to allow for accurate tracking of the person. A possible application could be the heating system, which safes energy by deactivating heating elements in rooms, where the user is not present in.

As the user returns back to the living room, both devices reside in the same room. In this case, there is no need to perform localization processes on either device until the user walks out of the living room or the handheld is picked up again, considering room-level accuracy.

1.5 Report structure

The thesis report is structured as follows. Chapter 2 surveys available indoor localization techniques and solutions to position and justify this work.

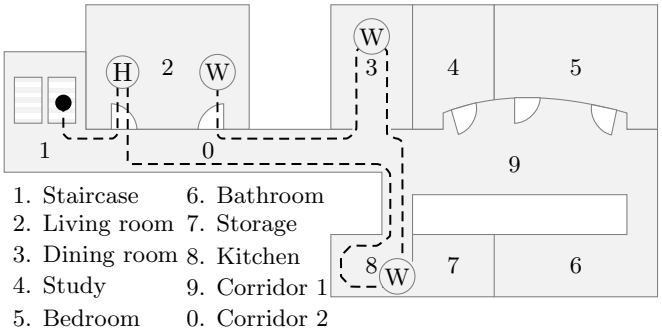

Figure 1.2: High-level overview of proposed system operation. The letter *H* indicates handheld location after being put down, while the letter *W* shows some of the wearable locations throughout the transfer.

Chapter 3 presents the general system overview and introduces the hardware configuration used for evaluation. Chapter 4 discusses design choices and limitations of the proposed method. In chapter 5 the system is evaluated by means of real-world experiments. Chapter 6 discusses the findings and limitations to assess feasibility of the proposed system. Chapter 7 concludes this work.

Chapter 2

Related Work

The Global Positioning system (GPS) accurately localizes users in the outdoor environment by means of satellite trilateration [18]. An indoor localization system as prevalent did not emerge yet from the numerous solutions suggested in literature. In the specific case of jointly using wearable and handheld, the latter can be considered part of a pervasive infrastructure, since its absolute location is known. For this reason, recent infrastructure-based solutions were surveyed in addition to infrastructure-free ones.

2.1 Indoor localization techniques

Common infrastructure-based techniques rely on on a number of different approaches including fingerprinting, geometric methods and proximity sensing. In advance, there is to say that terminology often differs. Infrastructure is referred to by different sources as access points, calibration points, beacons, receivers, and thus changes according to application and use. The term access point (AP) will be used to describe a single node of a localization infrastructure. Similarly, the line between infrastructure-based and infrastructure-free techniques has blurred by WiFi infrastructure being

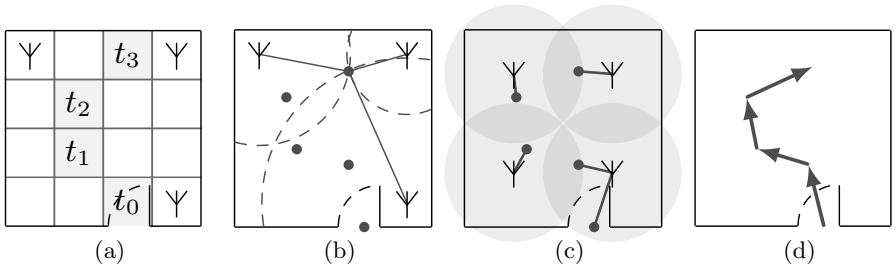

Figure 2.1: Common indoor localization techniques: (a) fingerprinting; (b) trilateration; (c) proximity sensing; and (d) pedestrian dead-reckoning.

partly considered as infrastructure-free due to its omnipresence. As there is no WiFi module present on the hardware configuration, the discussion can be avoided.

The fingerprinting technique is visualized in Fig. 2.1a and consists of two phases. In an offline phase a radio map of fingerprints is generated, associating ambient radio signals with physical locations. During an online phase, a device that observes the ambiance is able to collect a real-time fingerprint and compare it to the radio map entries using a pattern matching algorithm in order to estimate its location [19].

In the work of Calderoni *et al.* [20], such a base system is able to localise patients in a hospital environment. Patients are equipped with RFID transmitters; corresponding receiver access points store tag identifiers and RSS values. By using Random Forest classifiers, patient localization was performed correctly in 98 % of the cases with accuracy sufficient to distinguish between rooms. The area covered spans 4000 m^2 subdivided into 48 room and required a total of 9 access points. Clear advantage of the approach is the use of affordable RFID technology, which allows cost efficient scalability. However, the infrastructure required is generally not feasible for the target environment of a home or small office.

A specific approach to reduce the number of access points is proposed by Redvzic *et al.* [21] in the form of SEAMLOC. The Seamless Indoor Localization Based on Reduced Number of access points (APs) uses WLAN signals and requires up to 4 times fewer APs as compared to other approaches. A users location is interpolated in between APs based on probabilistic Bayesian functions by solving a system of two non-linear equations. The Naive Bayes method takes into account RSS and frequency of appearance of APs to achieve an accuracy of under 2.2 m on average. Nevertheless, the method is still unsuitable for localization when using only a single access point, due to high location ambiguity in fingerprints. Also, both approaches are generally prone to changes in the environment and rely strongly on unaltered conditions between offline and online phase to avoid recalibration.

A different approach is taken by Gao *et al.* [22], which concentrates on the aspect of power saving. ZiFind is presented, which exploits a cross-technology interface in the unlicensed 2.4 GHz frequency spectrum. With a low-power ZigBee interface it detects unique interference signature induced by the WiFi infrastructure and creates a fingerprint from it. A learning algorithm R-KNN is developed that classifies the location of a user based on a fingerprint database. The system has been deployed in a 16,000 ft^2 office with 28 rooms. The main drive behind developing ZiFind was developing the power saving feature by using the ZigBee technology.

And at last, the work by Wu *et al.* [23] approaches fingerprinting with the goal of eliminating the need for a site survey. It combines WiFi fingerprints with user movement related sudden changes in RSS on room change. A logical floor plan is constructed by assigning fingerprints to rooms. By

finding a match between the logical floor plan and a ground-truth floor plan, the user can be localized, without having to survey fingerprints in advance. The system achieves an average room-level accuracy of 86 %. The method still requires a number of APs to reduce ambiguity.

Geometric properties of triangles offer an alternative infrastructure-based localization approach. Triangulation measures the bearing relative to beacons placed in known locations [24]. Such direction-based techniques make use of the angle of arrival (AoA) or the angle of departure (AoD) to define arcs, whose intersection estimate a user's location. As neither wearable nor handheld holds an antenna array, direct angle measurement is not possible. However, in Fig. 2.1b trilateration, which is a ranged-based technique, utilizing received signal strength (RSS), time of arrival (ToA) or time difference of arrival (TDoA) information to infer a location, can be envisioned with a single handheld beacon, although resulting in high location ambiguity. In recent year no localization solution was proposed relying exclusively on geometric techniques.

For the sake of completeness it may be important to mention proximity sensing, where detecting spatial closeness of objects enables relative localization as shown in Fig. 2.1c. A device that is detected by an access point can be considered collocated with that access point. When a dense access point grid is present, it is considered to be collocated with the one receiving the strongest signal [25]. Similar to fingerprinting, the method is rendered unusable when having only a single handheld as access point. The obstacle of requiring a dense grid has lead to no implementations within the past five years utilizing this method exclusively. However, there has been an algorithm proposed to localize a target device in an indoor environment using energy efficient Bluetooth by Gu *et al.* [26]. It requires no access points or site survey, but explores Bluetooth characteristics. By interpreting Bluetooth RSS readings, the search space can be shrunk down until a target device is found. It achieves an average localization error of as small as 0.38 m, however, it does not allow absolute localization, due to a missing point of reference, but rather provides a tool to find missing bluetooth enabled objects within a single room.

On the other hand, infrastructure-free localization systems are well researched. Integration of inertial measurement units (IMU), commonly comprised of accelerometer, gyroscope and magnetometer, enable measurement of body-specific forces, angular rates and magnetic orientation of subjects. Using the infrastructure-free pedestrian dead-reckoning (PDR) methodology in Fig. 2.1d, the absolute location of a user can be determined by computing stride length, walking direction and integrating steps [27].

In the work of Kang *et al.* [5] a smartphone-based pedestrian dead reckoning system (SmartPDR) to track pedestrians is proposed. It uses data from inertial sensor embedded in smartphones. It is able to perform, step event detection, heading estimation, step length estimation, and location

estimation. It is able to achieve a localization error of 1.62 m solely based on smartphone sensors. Similarly Dead-Reckoning Enhanced with Activity Recognition (DREAR) is proposed by Torok *et al.* [4]. By nature PDR systems suffer from cumulative error introduced by the environment, but also by noisy sensors. Activities such as ascending and descending stairs, using the elevator or standing are used to recognize landmarks and increase precision achieving an average localization error of 3 m. DREAR requires a server side where data is processed which may cause privacy concerns. Clear advantage of PDR is the lack of required infrastructure. The need for a gyroscopic sensor prevents implementation on this work's hardware configuration.

2.2 Hybrid techniques

More common nowadays are hybrid systems made up of at least two of the methodologies in Fig. 2.1 in conjunction. In the work of Kumar *et al.* [6] a localization median error of 39 cm is achieved. The system called Ubicarse enables mobile devices to emulate a large antenna array to identify the spatial direction of incoming RF signals. It operates on of-the-shelf WiFi access points to perform triangulation. This information is used to improve noisy sensor data from accelerometer, magnetometer and gyroscope to estimate the antennas position. Later the camera of the mobile device is used for geotagging objects. The test environment being a library, with books arranged in shelves and racks, emulates multi-pathing. Using triangulation paired with a dead-reckoning approach, the system achieves sub meter accuracy. A drawback could be the large number of different sensors used and lack of evaluation for energy consumption, as a multitude of sensors are used simultaneously. Also, it would require multiple handheld devices and their location in the indoor environment to allow for simulation of the antenna array.

In the work of Wang *et al.* [16] unsupervised learning is employed to extract unique sensor signatures from locations (landmarks). Dead-reckoning schemes track location in between landmarks; once recognizing a landmark they re-calibrate their location. The system continues to improve localization accuracy over time. The approach does not require a specialized infrastructure, however, a ground plan of the building. It achieved a median error of 1.69 m online, however, is rather prone to changes in the ambience. Thus, being very similar to the approach in [4], the system tries to deal with an accumulated error in dead-reckoning schemes by using an access point infrastructure, rather than contextual information from the map.

This drawback of dead-reckoning has also been tackled in a similar way in the work of Abadleh *et al.* [28], who propose to use a physical map, rather than a radio map, in conjunction with smartphone sensors. It deals

with the accumulated error of a PDR approach by correcting the position with the position of a reference point. It utilizes a vector based motion model on a smartphone for direction and distance estimations. In addition, it uses RSS data of public access points to complement the PDR system. By representing the inner structure of a building as database relationship, the system achieves a mean error of 2 m and can perform floor discovery when leaving the elevator.

An approach specifically considering the computational efficiency is presented with the localization system MapCraft in the work of Xiao *et al.* [15]. It uses a graphical model known as linear chain conditional random fields (CRFs). It was found to be two to three orders of magnitude more computationally efficient than competing techniques. It uses a multitude of sensors including accelerometer, magnetometer and gyroscope for dead-reckoning, but also WiFi signals, Bluetooth, FM radio to estimate physical distances in combination with a ground plan. The system scales with the sensors available.

In the work of Hong *et al.* [14] a WiFi-Assisted Particle filter (WaP) is designed to improve dead-reckoning accuracy. It uses RSS readings by their contrast relationship, rather than absolute values, to perform turn verification, room distinguishing and entrance discovery. Although, it requrires a ground plan and AP locations, it achieves a localization error of 0.71 m efficiently with only several hundred particles and no interaction with a central server.

Also, a very promising approach has been taken by the work of Matiakakis *et al.* [29] with Single AP-based Indoor Localization (SAIL). To avoid a dense deployment of access points, manual fingerprinting and energy hungry WiFi scanning, it requires only a single AP in combination with smartphone sensor-based dead-reckoning using accelerometer, magnetometer and gyroscope. Using the propagation delay of direct path between smartphone and AP helps to eliminate multipath phenomenons, capturing a users location with a mean error of 2.3 m. The only drawback, is that it relies heavily on the orientation of a subject to determine how the user is transferring relative to the access point.

Table 2.1 summarises the surveyed localization solutions. It is important to note, that some hybrid solutions could not be clearly assigned to specific localization techniques anymore, as they were using small pieces of information of each technique. That also has to do with similarity among some techniques.

2.3 Justification

To summarize, while infrastruture-based techniques generally come with the obvious drawback of requiring an infrastructure, depending on technique

Table 2.1: Classification of surveyed indoor localization techniques.

Paper	a	b	c	d	Summary
[20]	✓				Equips patients with RFID tags and uses Random Forest classifiers
[21]	✓				SEAMLOC requires 4 times fewer calibration points based on bayesian probability
[22]	✓				ZiFind creates a fingerprint from interference signatures induced by WiFi infrastructure
[23]	✓				Creates a logical floor plan according to a user's movement and compares it to ground truth floor plan
[26]			✓		Explores Bluetooth characteristics to shrink down search space when searching another device
[4]				✓	DREAR uses landmarks to recover from dead-reckoning integration bias
[5]				✓	SmartPDR integrates steps, using heading and stride length
[6]	✓	✓			Ubicarse uses WiFi triangulation in combination with PDR and camera based geo-tagging of objects
[16]	✓			✓	Combines AP-based landmark calibration with PDR and uses unsupervised learning to improve over time
[28]	✓		✓		Uses PDR in combination with RSS data from access points for calibration
[15]	✓		✓	✓	MapCraft combined PDR and radio signal information using conditional random fields
[14]	✓			✓	WaP presents a WiFi-assisted particle filter-based PDR approach; it uses RSS by its contrast relationship
[29]	✓	✓		✓	Using geometric methods SAIL requires only a single WiFi access point in combination with a PDR approach

used, additional obstacles present themselves, for instance the offline calibration phase in fingerprinting systems. There has been a trend towards crowdsourcing this kind of information for instance by Zee presented in the work of Rai *et al.* [17]. It uses a dead reckoning approach in combination with a particle filter to localize users and take a fingerprint. The same goal has FreeLoc, which is presented in the work of Yang *et al.* [30]. It provides a reliable way to extract an accurate fingerprint from an RSS measurement lasting no longer than one minute. Real-world experiments using multiple mobile phones confirm that the proposed method requires no calibration among heterogeneous devices and resolves the multiple surveyor problem when crowdsourcing, which can provide a range of different fingerprints for the same location due to radio propagation phenomena. The need for a site survey could be eliminated entirely by the work of Wu *et al.* [23], which still brings along the drawback of requiring more than a single access point in the environment. An alternative, specifically discussing the problem of radio propagation phenomena presents the work of Yang *et al.* [31], which surveys Channel State Information (CSI)-based indoor loalization systems. Channel response systems are able to discriminate multipath characteristics and achieve centimeter-level accuracy, making them interesting for infrastructure-based solutions relying on the 802.11 a/g/n standards. As the standard is not available for the radio protocol used in the proposed system, it wont be pursued further.

As can be observed, the trend towards hybrid solutions is justified by obtaining an increasingly accurate IPS. However, complexity increases by crowd sourcing approaches and sampling of a multitude of sensors. Infrastructure requirements are present for fingerprinting, geometric methods and proximity sensing. On the contrary, there is limited attention given to the widely available and affordable fitness trackers, which make up a majority of wearables circulating and generally do not hold a gyroscope required for most PDR-based systems. These devices are generally not advanced enough for as complex hybrid solutions. According to this overview of localization methods, a system similar to SAIL in [29] will be proposed, requiring only a single access point in the form of the handheld. Given the radio's RSS, the distance can be used to calibrate a dead-reckoning approach. In addition a particle filter, which has been used in [14] and [17] is used to account for additional sensors noise and dead-reckoning bias.

Chapter 3

System Overview

In this section, some of the assumptions and design goals that lead to the system design are discussed. Furthermore, a conceptual overview of the system is provided.

3.1 Initial assumptions

The localization process of the system works in two different modes – (i) *standalone*, and (ii) *joint*. In *standalone mode*, only the handheld device is used for localization, whereas in *joint mode* both, the handheld and the wearable, are used. Since there exist a number of solutions that provide sufficiently accurate indoor localization using a handheld device, no new solution is developed for the *standalone mode*. Without loss of generality, a particle filter based dead-reckoning technique is adapted for the *standalone mode*, as used in [17]. As the major contribution is the joint localization system, the rest of the report will describe and evaluate the system only for the *joint mode*.

The floor plan of the indoor environment is assumed to be known beforehand. In addition, it is aimed for room-level accuracy, as it suffices for applications such as heating and lightning control [8]. Room size on the other hand may vary. As Bluetooth is the only radio interface on most wearables, it is used to communicate with the handheld. Due to the smaller form factor and limited battery capacity, wearables can accommodate only few sensor units. Thus, only an accelerometer and a magnetometer are present on the hardware configuration used.

The wearable should be non-intrusive: wearing more than a single device in uncommon body locations, such as the knees or feet, objects this requirement [32]. Hence, the system should run on infrastructure already present on the body. There are a number of common wearable locations, which are summarized in Fig. 3.2b. They clearly differ from common handheld locations in Fig. 3.2a. Each location will yield similar, but not identical sensor data. While the waist region may offer the clearest signal in regards

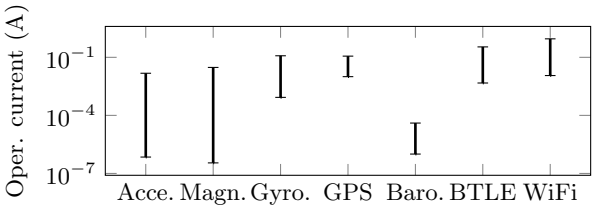

Figure 3.1: Comparison of sensor's energy consumption.

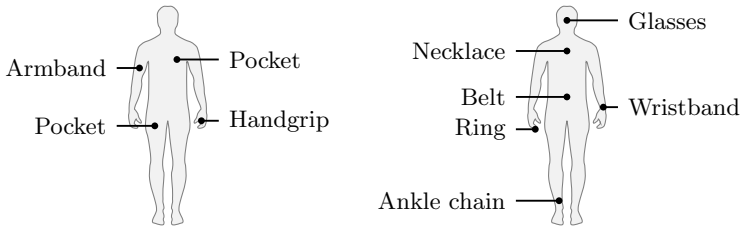

(a) Handheld body positions. (b) Wearable body positions.

Figure 3.2: Common and non-intrusive handheld and wearable positions on the body: (a) handheld; (b) wearable.

to human locomotion, a wrist-worn wearable is much more wide-spread [7]. For this reason, the wrist-worn wearable will be used as target device for this report.

3.2 Choice of sensors

In general accelerometer, gyroscope, and magnetometer are used in combination for step detection and heading estimation in dead-reckoning. As wearables do not feature all the three sensors (except few smartwatches), it is aimed to choose sensors that generally draw lower energy, and then try to optimize sampling intervals. Due to the wide range of operating currents of various sensor components, a direct comparison of energy consumption is difficult. Based on a survey of two major electrical component distributors [33, 34], it could be concluded that a magnetometer can provide more efficient operation than a gyroscope while acquiring heading information (see Fig. 3.1). In addition, a gyroscope requires continuous sampling to estimate heading direction. Additionally, integration of the gyroscope data is computationally intensive, and causes a cumulative bias error that is often difficult to rectify. Note that a magnetometer can also be biased by magnetic interferences in the indoor environment. However, it is expected to diminish this specific error by combining a Bluetooth RSS based distance measurement along with the dead-reckoning.

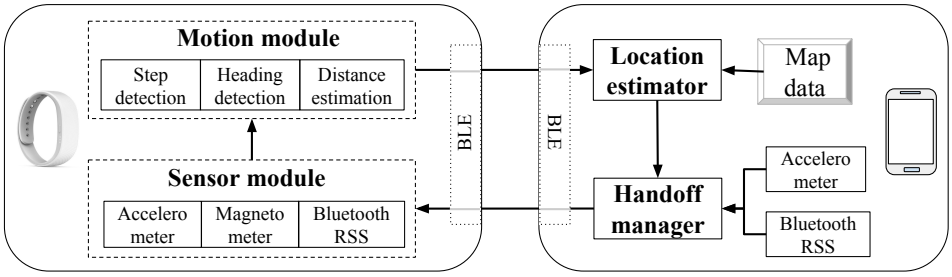

Figure 3.3: Overview of proposed system using both, the wearable and the handheld.

3.3 Design goals

The crux of the system proposed is to share the sensor load and processing tasks between handheld and the wearable in order to localize a person on a continuous basis. This amounts to the following two design goals. First, as the wearables have limited battery capacity, the usage of sensors has to be optimized towards energy efficiency without losing the required location accuracy. Thus, sensor sampling needs to be triggered only when it is required. Second, due to their restricted memory and processing capability, sensor data processing cannot be performed entirely by most of the commercial low-end wearables. Thus, some of the computational tasks need to be delegated to the handheld. However, keeping the energy constraint in mind, communication between the two devices also need to be kept at minimal.

3.4 Architecture

Fig. 3.3 depicts a pictorial overview of the systems architecture. By default, the localization process is executed on the handheld device in the *standalone mode*. The system triggers the *joint mode* by automatically detecting when the user moves around without carrying the handheld. As soon as the person starts roaming with the handheld, the process is switched back to the *standalone mode* and any localization-related activity on the wearable is stopped. In the following, the major building blocks of the system are briefly introduced.

Handoff manager. The selection of the localization mode is performed by the handoff manager running on the handheld. Its goal is to reduce energy consumption by avoiding unnecessary sampling of the sensors on both devices. It selects a suitable localization mode without incurring energy waste while ensuring a sufficient localization accuracy.

Sensor module. The sensor module resides on the wearable and switches the sensors on the device according to the handoff manager as well as ac-

quires the raw data.

Motion module. The motion module resides on the wearable. By processing the raw sensor data, it estimates three pieces of information about the user, that are, step event detection, heading direction, and distance from the stationary handheld device.

Location estimator. The location estimator resides on the handheld. It receives the motion model outputs from the wearable over the Bluetooth connection. It integrates this information with the map data using a particle filter based dead-reckoning approach. In addition using the distance information, the integration bias is supposed to be minimized.

3.5 Hardware configuration

Initially two different wearable devices were considered, both wristbands: the Samsung Gear Live is a Smartwatch with 1.63 inch display running the Android Wear operating system [35], the Xiaomi Mi Band is a fitness monitor without display [36]. Both communicate through Bluetooth 4.0 with a handheld application. Although these wristbands are representative for the type of currently available and affordable devices, their application program interfaces (APIs) were too limited for this work. The Bluetooth connection of the Samsung Gear Live is handled solely by the operating system. Things like reading out RSS were not possible, as no object for the Bluetooth adapter was present. The closed system of the Xiaomi Mi Band could not be programmed and flashed at all. Accelerometer data is processed onboard, and therefore, no raw accelerometer data could be retrieved either. Therefore, the decision was made to develop a wristband with similar specifications to the available devices.

For it, the choice was made to use a Bluetooth enabled System on Chip (SoC) solution by Nordic Semiconductor, the nRF52832, which was released March 2016. Bluetooth LE was favoured over Bluetooth Classic for a number of reasons: (i) Bluetooth LE was introduced in 2011 and has become the new standard in mobile devices; (ii) there is no audio streaming involved, which requires high throughput and low loss; (iii) long battery life on small batteries is necessary; (iv) cost is a concern [37].

The successor of the popular nRF51822 has been developed with two, at first glance contradictory, goals in mind: energy efficiency and computing capability. It is build around a 32-bit ARM Cortex-M4F CPU with 64kB RAM. In addition 512kB storage are integrated, which is sufficient for the envisioned localization system and makes an additional storage component obsolete. As the nRF51822 is an often used microcontroller in academia, industry and hobby, Tab. 3.1 provides a comparison of the the two chips, which may give some readers an indication of its performance.

The Accelerometer is the ADXL362 by Analog Devices, also used in the

Table 3.1: Comparison nRF51 and nRF52.

	nRF51	nRF52
CoreMark	2.33	3.40
Flash	256 kB	512 kB
RX current (3 V)	9.7 mA	5.4 mA
TX current (3 V)	8.0 mA	5.3 mA

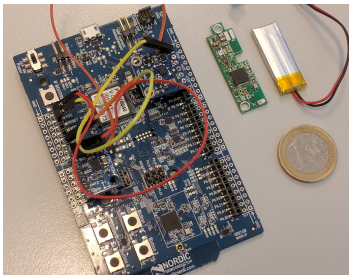

(a) Development board with wearable board next to it.

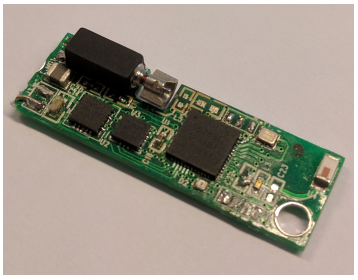

(b) Designed wearable board.

Figure 3.4: Hardware configuration of the wearable.

Xiaomi Mi Band. It has been chosen for its low current consumption of 1.8 μA at 100 Hz output data rate (ODR) considering a 2 V supply [38]. The magnetometer is the HMC5883L by Honeywell. It is an older model, even though labeled with low power consumption, it exceeds the accelerometer ones by far with its 100 μA.

From the available hardware components, two configurations were assembled. A prototype printed circuit board was designed to estimate the form factor and thus feasibility of the device. It can be seen in Fig. 3.4b with a width of 11.5 mm and a length of 39 mm. These dimensions are small enough to allow the wearable to rest comfortably on an average adult's wrist. As the process of developing the wearable board is of secondary concern, it has been left for a later point in time. Fig. 3.4a shows the development board (blue) next to the designed wearable (green). The development board provided by Nordic Semiconductors was used for all testing during development as well as evaluation. The accelerometer has been interfaced using SPI, while the magnetometer had to be interfaced using I^2C. The axes of both sensors were aligned accordingly. For this, in some cases remapping of axes was necessary.

Chapter 4

System design

In this chapter, the details of the system building blocks are provided (see Fig. 3.3). It is described how they work in synergy to achieve pervasive localization.

4.1 Handoff manager

The handoff manager is responsible for switching between the mutually exclusive *standalone* and *joint* localization modes (Fig. 4.1). The goal is to avoid sampling and data processing on wearable and handheld simultaneously and thus preserve energy. In general, handoff may take place when the user leaves behind the handheld and moves around. A trivial solution would be to trigger the joint mode as soon as the accelerometer data in the handheld suggests that the device is stationary. Similarly, switching back to the standalone mode is done, when the handheld becomes mobile again. However, this solution may lead to unnecessary switching between the two modes and hence superfluous sensor usage on the wearable. For example, when the user keeps the handheld on a desk and remains sitting next to it, the unnecessary handoff would cause energy drain on the wearable.

Since it is aimed for room-level accuracy, there is no need to handoff unless the user moves out of the *handheld room*, in which the handheld is located in and from which all wearable localization should origitate. However, if the handoff takes place only after the user moves out of the room, it takes a long time to determine the location of the user, especially in the case when there are multiple adjacent rooms to the *handheld room* due to slow particle convergence. Given the particle filter based localization technique, it was determined that correct and expeditious particle convergence can be guaranteed, when the handoff to *joint mode* takes place before transferring to an adjacent room.

The system uses a dynamic approach to make the handoff decision, i.e., switching between the two localization modes. The handheld's accelero-

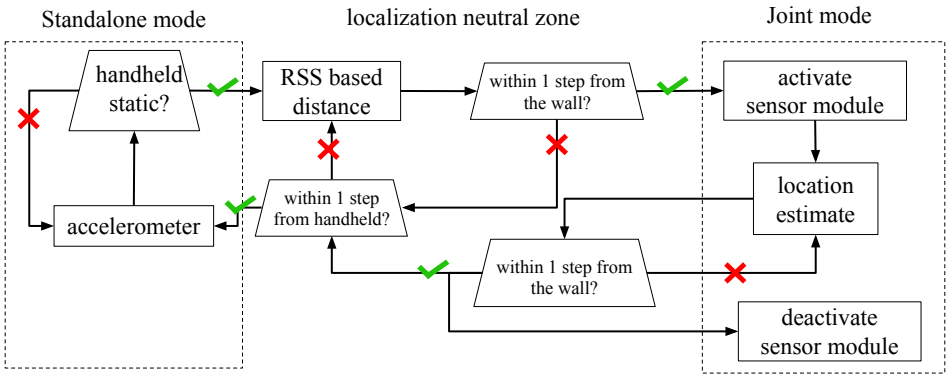

Figure 4.1: Switching between the two localization modes by the handoff manager.

meter is leveraged to detect motionlessness, which is a good indicator for the handheld being left behind. At this point, the location of the user is the same as the handheld room, and the localization process enters a *localization neutral zone*. Using contextual map data, the distance between the handheld's absolute location (based on *standalone mode*) and the closest wall to an adjacent room is determined. This distance determines the *upper* dynamic handoff threshold. Depending on the RSS of Bluetooth, the distance to the wearable is estimated. Once the user crosses the handoff threshold distance, the joint mode is triggered.

To switch back to *standalone* mode, the wearable needs to return into close proximity of the handheld, where the distance between them has to be less than a *lower* predefined handoff threshold. RSS measurements are tight to the synchronous connection interval of the Bluetooth connection, which is present throughout. Distance measurements can therefore be performed by both devices, wearable and handheld. In Fig. 4.1 there is a reference used to a single step from either the wall or the handheld to make the handoff decision. Depending on the accuracy of the RSS this distance can be adjusted, which will result in the location neutral zone either growing or shrinking in size.

4.2 Sensor module

The sensor module in the wearable receives a trigger from the handoff manager when the switching to *joint mode* takes place. for this, the handheld sends a message to the wearable over the Bluetooth connection. Only at this point, the accelerometer and the magnetometer units are activated on the wearable. The sampling rate for the accelerometer is set to 20 Hz as this is the minimum required rate to identify frequencies in human locomotion, including steps accurately [39]. However, the magnetometer is not sampled

at a fixed frequency. Rather it is sampled in an event driven manner, every time when a step is detected by the motion module. The details of step detection by the motion module based on accelerometer data are discussed in Section 4.3. Additionally, the Bluetooth RSS is measured on the wearable to calculate the distance from the handheld. This helps to estimate the location of the user.

4.3 Motion module

The motion module receives the data from the sensor module, processes it, and provides three pieces of information – (i) when a step is detected, (ii) what the heading direction of the user is, and (iii) what the distance between the user and the handheld is.

Step detector. There exist a number of freely accessible accelerometry-based step detection algorithms, which have been compared by Marschollek *et al.* [40]. However, these algorithms are generally envisioned to process accelerometer data obtained from a waist-belt. On the other hand, wrist-worn and non-freely accessible algorithm by wearable manufacturer have been around for a few years as well. As step detection is not the primary focus of this work, and there seems to be no need for extensive research, a simplistic threshold based algorithm will be used as in Alg. 1.

Algorithm 1 Step detection and counting algorithm on Wearable

Input: $\vec{a} = \begin{bmatrix} a_1 & a_2 & a_3 \end{bmatrix}$
Output: steps
SAMPLE Process
if $|\vec{a}| > threshold$ **and** $flag == 0$ **then**
  steps++
  $flag == 1$
end if
return steps
Timer Reset Process
if $flag == 1$ **then**
  wait average step duration..
  $flag == 0$
end if

Each time when the accelerometer data is sampled, total acceleration is calculated by computing the magnitude from three axis components. If this magnitude crosses a predefined threshold, it is considered as a step. Once the step is detected, the sampling is paused for a small duration roughly equalling the duration of an average step. This avoid multiple (false) step detection within the same step period.

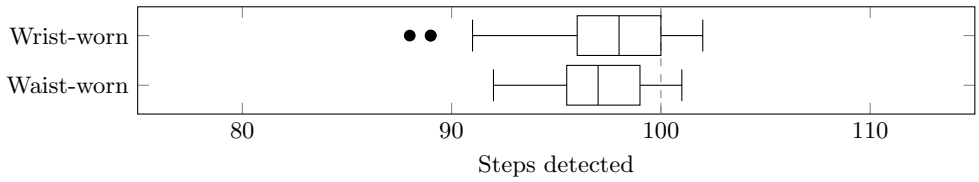

Figure 4.2: Step detection capability for 100 consecutive steps taken.

The algorithm has been tested on two users with different height, and gender. The tests are conducted for two different locations of the wearable – waist and wrist. From the results summarized in Fig. 4.2, it can be concluded that the algorithm achieves a reasonable accuracy. Note that one of the drawbacks of this technique is that any acceleration value crossing the threshold (due to other activities) would be considered as step. However, the goal is not to detect the step with highest accuracy, but use it for localization. The localization algorithm has to show enough robustness to deal with miss-detection of some steps.

Heading Detection. When estimating the heading of the owner it is relied on two assumptions. First of all the wearable is worn on the wrist. Secondly, while walking, the owner swings her/his arms parallel to the body. Thus the wearable swings in walking direction back and forth. A magnetometer alone cannot detect heading under these circumstances. Hence, a tilt compensated compass using magnetometer and accelerometer is necessary. For it, an accelerometer sample, which gives an indication of the gravity vector $\boldsymbol{a} = \begin{bmatrix} a_x & a_y & a_z \end{bmatrix}$ and a magnetometer sample, a vector pointing to magnetic north $\boldsymbol{e} = \begin{bmatrix} e_x & e_y & e_z \end{bmatrix}$ are acquired. In order to construct a coordinate system, a third vector perpendicular to both of these vectors is computed by using their cross product: $\boldsymbol{h}$ and its unit vector $\hat{\boldsymbol{h}}$ are computed.

$$\boldsymbol{h} = \boldsymbol{e} \times \boldsymbol{a};\ \hat{\boldsymbol{h}} = \frac{\boldsymbol{h}}{|\boldsymbol{h}|} \tag{4.1}$$

The accelerometer and the magnetometer vectors are generally not perpendicular due to earth's spherical shape and location dependent inclination, the process of finding a better axis representation for magnetic north has to be repeated. The unit vector $\hat{\boldsymbol{a}}$ is found to compute $\hat{\boldsymbol{m}}$.

$$\hat{\boldsymbol{a}} = \frac{\boldsymbol{a}}{|\boldsymbol{a}|};\ \hat{\boldsymbol{m}} = \hat{\boldsymbol{a}} \times \hat{\boldsymbol{h}} \tag{4.2}$$

This vector is already a unit vector, because $\hat{\boldsymbol{a}}$ and $\hat{\boldsymbol{h}}$ are. For completeness the corresponding change of basis matrix $\boldsymbol{R}$ is presented.

$$\boldsymbol{R} = \begin{bmatrix} \hat{h}_x & \hat{h}_y & \hat{h}_z \\ \hat{m}_x & \hat{m}_y & \hat{m}_z \\ \hat{a}_x & \hat{a}_y & \hat{a}_z \end{bmatrix} \tag{4.3}$$

Using the by programming languages defined function atan2(h_y, m_y), the heading in radians is acquired by using the signs of the vector components h_y and m_y. Due to the use of an accelerometer, the heading is tilt-compensated and even when the hands are swung back or forth gives a reliable heading. The heading, which is stored as 4 bytes floating point number, is computed with a new magnetometer sample whenever a step event occurs, in order to limit sensor sampling.

Distance estimator. Though RSS-based distance estimation in the indoor environment can be erroneous, it is used as a secondary mechanism. As the dead-reckoning is also subject to error, the RSS-based distance estimation is used to calibrate during the localization process. How these two error-prone technique complement each other to establish accurate location information is described in Section 4.4.

As the devices are paired using Bluetooth, the RSS, which represents the relationship between transmission and received power, can give an estimate of their distance. Eq. 4.4 presents a common approach towards distance estimation for the received signal strength S in dBm [41].

$$S = -10\eta \log_{10} d + A. \tag{4.4}$$

Here, η is the propagation path-loss exponent ($\eta = 2$ for free space), d is the distance between the sender and the receiver in meters and A is the received signal strength at one meter of distance.

To decide an appropriate path loss exponent for the given indoor environment, RSS was measured with increasing distance between the handheld and the wearable. When the devices were in line-of-sight in a long corridor, the resulting path loss exponent is at times less than 2 (Fig. 4.3a). The reason behind this is that a long corridor may resembles a tunnel, which may act as wave guide, providing a stronger signal at a relatively shorter distance [42]. The measurements confirm the observations made in the work of [43] as RSS being rather unreliable. Furthermore, it has been found empirically that a wall reduces the signal power by approximately 3 dBm (depending on wall type and construction) [44]. In subsequent measurements with walls and furnitures in the path a stronger down-trend of the resulting signal was observed, indicating a higher signal attenuation. In such cases, a better approximation of the loss exponent is $\eta = 2.5$ (Fig. 4.3b).

In order to cope with the deviation, a low-pass filter was implemented, which cancels out high frequency noise to estimate the distance d more accurately.

$$d = \alpha \times d_{t_{-1}} + (1 - \alpha) d_{t_0}; \tag{4.5}$$

Note, that the distance d is smoothed out, rather than the RSS value directly. The reason is that the RSS is in a logarithmic relationship to the distance. Therefore, smoothing the RSS directly may result in changing responsiveness of the system at different distances between handheld and wearable.

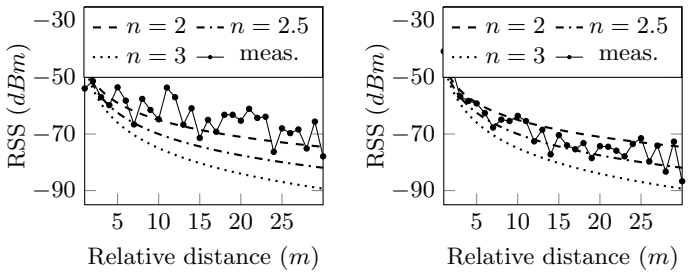

(a) Corridor acting as waveguide. (b) Obstructing walls.

Figure 4.3: Relative distance of devices and corresponding RSS [45]: (a) free-space measurement; (b) measurement with obstructing walls and furniture. The experimental η is updated and adapted for different indoor environment.

4.4 Location estimator

To estimate the location of the user, the system integrates the information received from the motion module with the map data using a particle filter. The particle distribution is initiated when the *joint mode* is triggered by the handoff manager. As the user walks further, the particle positions are updated using two sequential mechanisms: first, dead-reckoning, second, distance-based calibration. As dead-reckoning is prone to cumulative errors, the RSS-based distance is used to rectify this error.

To expedite the particle convergence initial particle distribution is done judiciously. As mentioned in Section 4.1, the handoff takes place when the user moves beyond the threshold distance from the handheld; but still resides in the same room. Considering the handheld room as the initial location, all the particles are distributed within this room. However, if particles are distributed all over the room, they may form multiple clusters if there are multiple exits from this handheld room. To tackle this issue, the particles are projected in an arc with mean being the heading direction θ plus the heading noise introduced into the system.

Similar to the work in [17], each particle is represented using a 2D co-ordinate on the floor map, where particle i at step k has coordinate (x_i^k, y_i^k). If the user is heading at an angle of θ, and the stride length is s, then, each particles' location is updated with each step according to the following equations.

$$x_i^{k'} = x_i^k + (s + l_i^k)\cos(a_i^k + \theta) \tag{4.6}$$

$$y_i^{k'} = y_i^k + (s + l_i^k)\sin(a_i^k + \theta), \tag{4.7}$$

Here, l_i^k and a_i^k are the stride length noise and heading noise respectively, which are deliberately added to the system to account for unreliable RSS as well as heading estimate. As a result, the particles are relocated to any

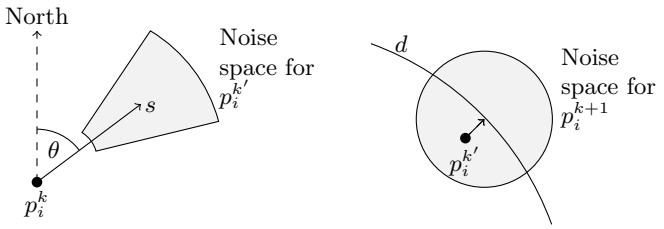

(a) dead-reckoning based relocation. (b) device distance based relocation

Figure 4.4: Noise added during particle relocation to catalyze convergence.

location within a determined region as shown in Fig. 4.4a. This noise is also added to catalyze the particle convergence as well as provide recoverability from location errors. The noise values are chosen from uniform distributions where s and θ are the mean of the distributions. The range of the distributions are selected experimentally and discussed in Section **??**. Next, device distance-based calibration is performed, which can eliminate the integration error caused by the dead-reckoning. It projects particles into a location corresponding to the distance d between the devices (Fig. 4.4b). The value of d is calculated by the distance estimator based on the RSS value received at the wearable. To do so, the coordinate $(x_i^{k'}, y_i^{k'})$ of a particle $p_i^{k'}$ are transformed from the map coordinate system to a coordinate system centered at the handheld's location (x_0, y_0) and the length of the resulting vector $\boldsymbol{u_i}$ is computed.

$$\boldsymbol{u_i} = (x_i^{k'} - x_0, y_i^{k'} - y_0) \tag{4.8}$$

$$|\boldsymbol{u_i}| = \sqrt{{x'}_i^2 + {y'}_i^2} \tag{4.9}$$

This vector is scaled to have length equal to the radius of the distance sphere, resulting in $\boldsymbol{v_i}$.

$$\boldsymbol{v_i} = \frac{d}{|\boldsymbol{u_i}|}\boldsymbol{u_i} \tag{4.10}$$

Finally, the vector can be scaled back to the map coordinate system to get the projection pointed to by the vector $\boldsymbol{w_i}$.

$$(x_i^{k+1}, y_i^{k+1}) = \boldsymbol{v_i} + (x_0, y_0) \tag{4.11}$$

At last, uniformly distributed noise is added by further relocating the particle p_i randomly within a spherical noise space with radius n around the projected point (Fig 4.4b). This accounts for the unreliable RSS value as well as diminishes the bias introduced by the projection of a particle.

The newly acquired location is then validated, i.e., whether it is outside the mapped area or if the line joining (x_i^k, y_i^k) and (x_i^{k+1}, y_i^{k+1}) intersects a wall on the map. In such cases, the particle is eliminated and resampled in a valid and randomly chosen particle's location at the previous step.

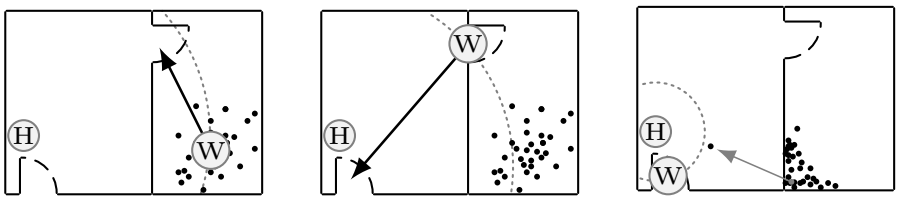

Figure 4.5: Working principle of deadlock discrepancy check: (a) step events go undetected by wearable; (b) particles are left behind; (c) recovery of a particle.

During tests an undesirable particle behaviour was observed. It may occur that particles get locked into corners. This is commonly encountered in PDR systems and is a result of integration bias or falsely detected step events. In the exceptional case, that every single particle is trapped within a corner, a deadlock can occur. The particles will be destroyed and resampled in the locked location. To account for this a check is performed on a single randomly chosen particle. It's distance to the handheld is compared to the distance computed from the RSS. If the discrepancy is too large, the particle will be allowed to surpass wall restrictions. This will only be granted to a single particle to avoid discrepancy checks of multiple particles, and thus, recovery may take a few steps. This process is visualized in Fig. 4.5

Chapter 5

Evaluation

This section presents the performance evaluation of the system in regards to location accuracy, computational complexity and robustness of the localization process, and efficiency of the handoff mechanism. The evaluation has been performed in an indoor environment spanning about 320 m^2. Fig. 5.1 shows the floor plan of the area, which is split into 10 rooms. The central corridor including the staircase has an end-to-end distance of about 30 meters. While Bluetooth has a theoretical range of more than 100 m, the practical communication range is significantly less, especially in the indoor environment. However, the longest distance in the experimental area was found to be barely within the communication range of the wearable device given the environments radiopacity. It is worth noting that reconstructable disconnects of the Bluetooth connection could be forced for some room pairs of handheld and wearable, when moving into far ends of certain rooms.

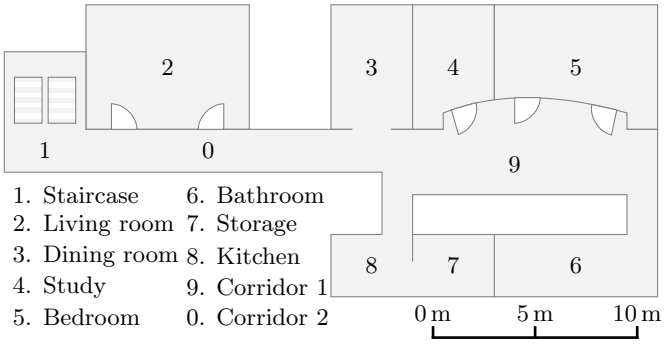

Figure 5.1: Floor plan of the indoor environment that is considered for calibration and testing of the proposed system.

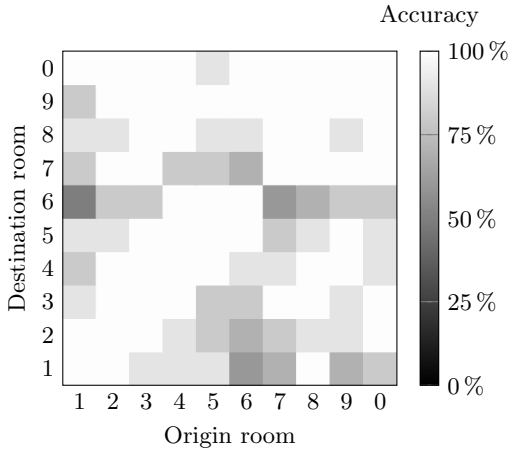

Figure 5.2: Confusion matrix of individual room transfer accuracies.

5.1 Accuracy

As a room-level accuracy is sufficient in most of the indoor living spaces, the primary target of the system is to achieve such an accuracy. First, it was tested whether the system is capable to determine the location and the transfer of the user within the test environment. For this, the transfer accuracy for a limited number of room pairs is evaluated. Fig. 5.2 summarizes the results of this evaluation, which are an average of ten experiments for each room pair. Though, most of the room combinations (origin and destination room) show accurate location estimation, there are a few cases where the accuracy is below average (generally involving rooms *1*, *6*, and *7*).

Classifying transfer accuracy contextually by absolute room distance reveals that localization accuracy decreases with increasing distance from the handheld room (Table 5.1). As RSS-based distance estimates gets hampered with larger distance, the localization accuracy also decreases at far ends of the indoor environment. In addition, the lower accuracy involving rooms *6* and *7* can be explained by the density of the area. While the width of the walls in between rooms *2* through *5* are almost similar (about 10 cm), rooms *6* and *7* can only be accessed through small corridors, that are heavily concrete reinforced. Hence, the un-uniform density of an indoor environment creates low accuracy for the proposed localization system.

Next, it was experimented with ten people of varying age, height, and gender. The users were asked to transfer randomly between rooms considering two different handheld locations (handheld rooms) for each of them. The location of the handheld, i.e., the initial location of the user is determined using the *standalone mode* and not included in this evaluation.

The experiments started after the handheld is kept on a table in the handheld room. At this point, the system enters the localization neutral

Table 5.1: Accuracy by room distance.

Room distance	Accuracy
<10 m	96.91 %
<20 m	93.54 %
<30 m	91.20 %

zone. As the user moves away from the handheld gradually, the handoff takes place and the localization in *joint mode* starts. As mentioned earlier, the handoff takes place based on the dynamic handoff threshold distance, which is decided based on the distance between the nearest wall and the handheld in the handheld room. As the user moves from room to room, the location is also updated accordingly. Note, that the handheld room is not kept fixed. Based on a total of 350 room transfers, the system achieves a localization accuracy of 90.31 %.

5.2 Particle filter optimization

The computing load is distributed over the handheld and the wearable, however, not evenly. Both the devices are limited in processing capability and power supply, with the handheld being generally more capable. Therefore, the particle filter has been chosen to run on the handheld, whereas the wearable provides the required information to update the particles based on the sensor data. However, to avoid unnecessary processing and memory consumption, the particle filter can be optimized by limiting the number of particles. On the other hand, more ambiguity can be rectified with an abundant number of particles. Thus, there is a clear trade-off between the number of particles and accuracy.

However, first the noise added to the system during the particle relocation is evaluated (see Fig. 4.4) with an abundant number of particles. The various noise levels that are used in the experiments are quantized in Table 5.2. As mentioned earlier, stride length noise and heading noise for the dead-reckoning approach is introduced. The distance noise n has been predetermined to be $3s$. This measure is retrieved from the floor plan and can slightly vary for different indoor environments, depending on size of rooms and density of room entrances. The distance noise resembles the radius of a sphere, which just barely fits in the smallest room on the floor plan (room *7*). It distributes the particles as much as possible, without allowing too much leakage to the adjacent room, e.g., room *8*. All noise is uniformly distributed. The use of a specific probability distribution is deliberately avoided, to maintain the independence of the particles from one another, and thus avoid artificially forced particle convergence. The noise is chosen

Table 5.2: Noise quantification.

Noise level	Stride length (s)	Heading (θ)	Distance (n)
0 %	s	θ	$3s$
25 %	$s \pm 0.25s$	$\theta \pm 11.25°$	$3s$
50 %	$s \pm 0.5s$	$\theta \pm 22.5°$	$3s$
75 %	$s \pm 0.75s$	$\theta \pm 33.75°$	$3s$
100 %	$s \pm s$	$\theta \pm 45°$	$3s$
125 %	$s \pm 1.25s$	$\theta \pm 56.25°$	$3s$

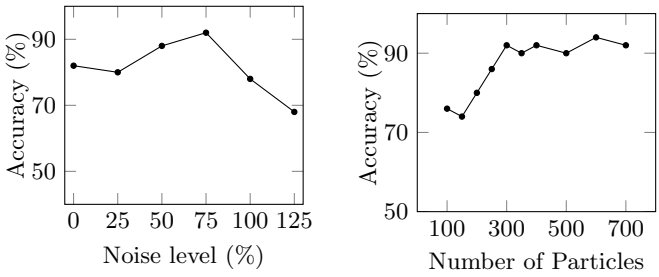

(a) Optimizing amount of noise. (b) Optimizing amount of particles.

Figure 5.3: Particle filter optimization.

in relation to a person's stride length s. Average stride length has been found to be about 75 cm, though it mostly varies based on the height of the user.

Fig. 5.3a summarizes the localization accuracy against various noise levels. Though, there is no observable clear trend, the performance seems to be peaked at the noise level of 75 %. After that, performance seems to decrease with higher noise levels. This could be caused by the noise space for the heading angle getting too wide, as well as stride length varying too drastically between particles. Data suggests that it cannot be concluded with certainty, that the noise levels below 75 % are not entirely unsuitable. However, it was decided to use said noise level as default for all the evaluations.

When testing accuracy of the localization process with respect to the number of particles it could be concluded from Fig. 5.3b that at least 300 particles are necessary to provide good accuracy. This value may vary depending on the factors such as the average room size of the indoor environment and the number and distance of room entrances. However, for all experiments, a number of 300 particles was adopted.

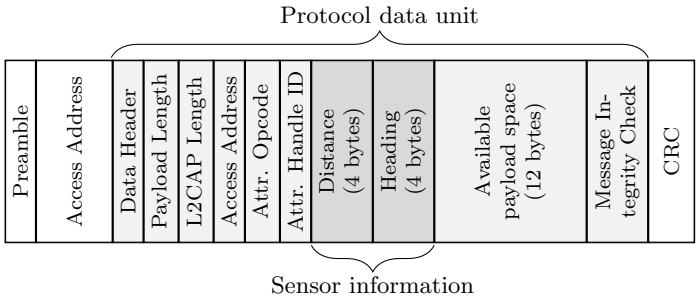

Figure 5.4: Bluetooth packet as used for transmission during *joint mode*.

Table 5.3: Packet loss simulation.

Packets missed	Accuracy
0	90.31 %
1	74 %
2	66 %
3	<50 %

5.3 Bluetooth communication

The necessity to fit all data sampled at a step event into a single Bluetooth package arises from the requirement to limit Bluetooth transmission to preserve energy. Distance and heading estimations are stored as floating point values, each of them 4 bytes long. Therefore, all the data from a single measurement are transported in a single packet (Fig. 5.4).

As communication incurs additional energy consumption, a less frequent packet transmission would be energy efficient. However, it may severely impact the localization process. To study this impact, packets are sent with larger intervals, i.e., instead of sending packets at every step detection, a packet is sent only on every second, third and fourth step. This provides incomplete information to the particle filter. Even though, the system seemed to perform reasonable for missing every second step while transferring within the corridor (room *0* and *9*), it more often missed out on the smaller rooms. The distance-based calibration shows its usefulness by interpolating the distance traversed when packet loss occurs. The accuracy further degrades with more missing steps as is summarized in Table 5.3.

The results signify that even if steps are missed every once in a while, it would not introduce an unrecoverable error. In fact, the RSS-based calibration aids such scenarios when packets are lost or steps go undetected, as it calibrates the particles onto the most recent distance. Decreasing communication rate by default is not advised as it decreases accuracy accordingly.

Table 5.4: Energy consumption of system activities.

Activity	Abbrev.	Consumption
Bluetooth connection	BTLE	10 μA
Handheld accelerometer	HA	3 μA
Wearable accelerometer	WA	3 μA
Wearable magnetometer	MAG	100 μA
Transmit packet	TX	2 μA

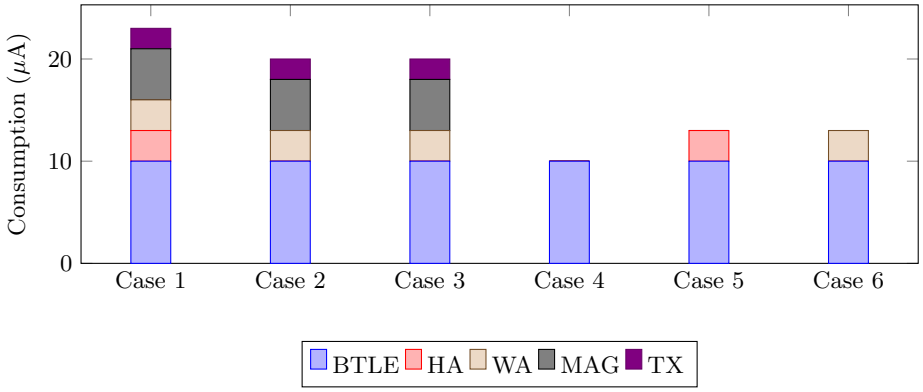

Figure 5.5: Energy saving for handoff related cases.

5.4 Hand-off

Switching from *standalone mode* to *joint mode* is crucial, because on handoff the particles are projected into the heading direction of the user. If projection happens in the wrong direction for a specific handheld room with multiple exits, recovery will not happen unless the user returns to this handheld room. This handoff mechanism has been evaluated in Fig. 5.2 as well. It uses the transfer accuracy through an exit from the handheld room to an adjacent room. This transfer was successful in 97 % of the cases. Handoff accuracy directly contributes to the overall accuracy within 10 m of range from the origin room.

Averaged theoretical component power consumption of the hardware configuration is summarized in Tab. 5.4. It is important to note that maintaining the Bluetooth connection also enables reading out RSS. Given a number of cases the current consumption of the system differs (Fig. 5.5).

Case 1. No handoff mechanic is present. Handoff related handheld sensors as well as all wearable sensors sample continuously.

Case 2. No handoff mechanic is present. Handoff related handheld sensors as well as all wearable sensors sample continuously. Because *standalone* mode requires an accelerometer as well, the system is free-riding.

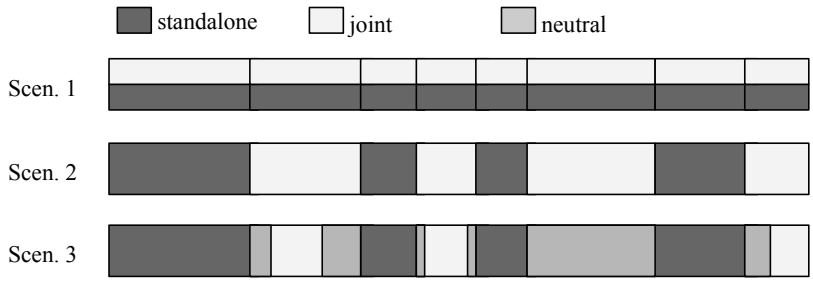

Figure 5.6: Evaluation of handoff modes.

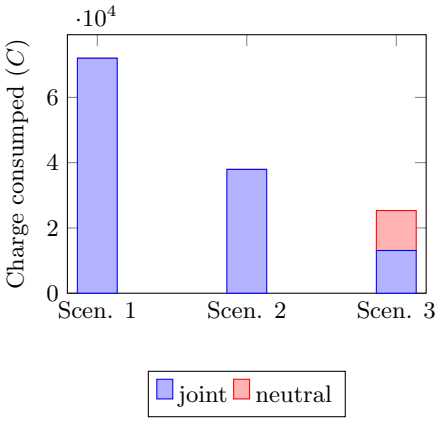

Figure 5.7: Energy consumption of wearable.

Case 3. The user is transferring in between rooms, while *joint* mode is active.

Case 4. The wearable transfers within the *localization neutral* zone.

Case 5. The user resides within 1 steps of the location of the handheld.

Case 6. The user rest on a chair while *joint* mode is active.

Handoff mode offers possibilities to safe energy, considering that the sensors are significantly more energy demanding than the energy necessary to maintain a Bluetooth connection.

To evaluate the room for energy saving further, Fig. 5.6 presents three scenarios in which a user switches between the *standalone*, *joint* and *neutral* localization modes. Each time *standalone mode* makes up 47.3 % of the overall duration of the scenario and *joint mode* makes up 52.7 %. The absolute duration of the scenario is one hour. In Scen. 1, both these modes are active continuously. In Scen. 2, a handoff takes place when mode changes. In Scen. 3, the handoff is complemented by the *neutral mode*, which takes a place in between the other two modes. That means 34 % of the entire duration are taken up by neutral mode, which corresponds to 65.5 % of the time *joint mode* should have been active.

The results in Fig. 5.7 suggest that there is a benefit to the handoff mechanism. If the wearable would be active throughout as in Scen. 1, the energy would deplete about twice as fast as with separate modes for *joint mode* and *standalone mode* as in Scen. 2. Scen. 3 shows the benefits of the handoff mechanism and the *localization neutral* mode. which decreases charges consumed even further as compared to Scen. 2.

It becomes apparent that the benefit of the handoff mechanism cannot be easily modeled. It depends greatly on the behavior of the user and can thus vary between almost non existent and clearly present. The energy required to keep the two devices connected diminishes the benefit of the handoff mechanism and makes it additionally highly dependent on the currents consumed by the sensors.

5.5 Scalability

The survey in [25] mentions the scalability character as an important aspect of a localization system, since location capability has to be guaranteed even if the positioning scope gets large. It becomes apparent that the proposed localization system in the current form is unable to scale on neither of two axes: geography and density, because merely a single pair of wearable and handheld is considered. According to [25] geographic scale describes the area or volume covered, while density scale describes the number of access points located per unit geographic area. Therefore, deployment of the system is only feasible in indoor environments, where end-to-end distances do not cause disconnects and provide reliable RSS values considering present radiopacity.

Chapter 6

Discussion

This chapter discusses the results obtained from the evaluation as well as the limitations of the system to conclude its overall feasibility for the purpose of pervasive service provisioning.

6.1 Limitations

In the preceding chapters, limitations of the system have been pointed out occasionally. As some of them may be crucial to the systems feasibility, this section summarizes the important ones once again.

Radio propagation phenomena. The radio connection between handheld and wearable is based on the Bluetooth protocol operating at 2.4 GHz. While the speed of theoretical 25 Mbps may be less of a concern, the range, which is device-based, depends strongly on the radiopacity of the indoor environment. In the rather lossy test environment with a limited number of furnitures, that are mainly chairs, desks and computer equipment and thin walls (from glass or synthetic material), close to optimal requirements are simulated. This also diminishes the effect of multipath, because the waves can penetrate objects easier. The significant drawback has become apparent from the rooms *6*, *7* and *8*, which are hidden behind heavily concrete enforced walls with metal components for an elevator shaft. Entering these rooms was generally detected correctly, however, afterwards the distance was often highly overestimated, leading to false detection of following locations and particle deadlock. For this reason, during evaluation, the users were asked to not move to the far ends of these specific room, but rather remain at their entrance and center areas.

External heading noise. The heading of the user is computed from the alignment of the sensors in regards to magnetic north. As the sensor is fixed to the wearable, the wearable orientation becomes important. The tilt compensation is able to filter out vertical offsets, which are commonly introduced by the arm swing. However, tilt-compensation relies also on the

accelerometer data to find the gravity vector, which may be biased due to the accelerations introduced by the arm swing itself. That means that a strong arm swing can cause greater heading offsets than smaller ones. During evaluation the users have been, to some extend unnecessarily, careful with the wearable and thus the effect was not observed within the large amount of deliberately added noise, however, it clearly persists. The simplest, but also most unreliable, solution to this is to use a low-pass filter, which filters out the high frequencies from the arm swing. The Android API uses sensor fusion with a gyroscope to provide a virtual sensor, which unfortunately is not present on the proposed system. In additon to this, noise can be introduced by any sort of hand gesture during walking. Clearly, this will immediately give an incorrect heading and lead to inaccurate localization. Orientation independent heading estimators while walking have been proposed in literature in [46], [47] and [48] for smartphones in the pocket. The idea is to project the acceleration from the sensor into the horizontal plane by means of a change of basis matrix. The heading can then be deducted from the gait cycle, as there will be accelerations towards the walking direction. However, this requires a constantly updated change of basis matrix, which again requires a gyroscope and significant processing capability. On the proposed systems such solutions are currently not feasible. Thus, any noise introduced other than the arm swing will cause inaccurate localization.

Magnetic field noise The magnetic noise introduced by electric appliances and metal objects in the indoor environment has not been considered specifically. The magnetic field noise in the test environment was present but, considering room-level accuracy, did not appear to be of concern. As this noise has not been quantized, it is not possible to tell how the proposed system would perform in other indoor environments.

6.2 Feasibility

Given the evaluation results as well as list of limitations the question arises if the proposed localization system is feasible to achieve pervasive localization. Personally, I see the main contribution in the notion of using wearable and handheld in conjunction. To the best of my knowledge, such a distributed system using two pervasive interface devices has not been proposed in the past to achieve indoor localization. I am convinced that it presents a viable system setup also for future work. The addition of a handoff mechanism shows energy benefits, which, however, appear less significant next to the energy consumption for maintaining a bluetooth connection. Especially in this regards, energy saving depends strongly on the efficiency of the sensors used, and in the presented case, falls short of expectations. The average localization accuracy of about 90 % seems competitive to some approaches aiming for room-level accuracy, such as [23], which achieves 86 % accuracy,

however, lags behind the work in [20], which achieves 98 %. But, looking at the hidden numbers of the confusion matrix in Fig. 5.2 reveals that localization accuracy for some room pairs was observed to be as low as 50 %. This mainly concerns rooms behind concrete walls, which can be very common. Providing a location-based service only every second time a specific room is entered is not practical and unacceptable for all parties involved, provisioners as well as recipients. The main contributor to this error seems to be the RSS. It's unreliability has been underestimated in the first place and due to the sequential resampling of particles, it is given too much weight during localization. Possible options are to improve it in one way or another to take into account phenomenons such as multipath, or replace it entirely.

6.3 Future work

A number of techniques may improve localization accuracy of the proposed system in the future.

Bluetooth 5.0. It is expected that with the announcement of Bluetooth 5.0, the technology may get back to the spotlight for indoor localization solutions. The standard promises to quadruple the range and double the speed of Bluetooth 4.2, which is the most recent version.

Kalman filtering Currently the dead-reckoning as well as the distance information are processed sequentially, generally resulting in the distance information being weighted more. By implementing a Kalman filter, the two mechanisms could be fused and it would be easier to detect and account for large errors in either of the two. For example, large RSS deviations can then be taken into consideration with diminished weight.

Hardware antenna tuning. The RSS appeared to be main cause for errors in the system. The read out value is highly dependent on the quality of the antenna circuitry. The nRF52 chip is able to read out RSS in a significantly higher resolution than the handheld employed for evaluation. A study on how accurate the RSS value is in other devices would give an indicator of how feasible the overall idea is.

Improve scalability factor. Instead of utilizing only a single pair of wearable and handheld, there may be the possibility to use a number of handheld devices of colleagues or room mates. The feasibility of such an approach can be researched as it may improve scalability of the system to provide coverage over larger areas.

Chapter 7

Conclusion

Indoor localization is an important enabler of pervasive services. As handhelds are generally not carried continuously in non-public indoor environments, the necessity for a wearable-based localization system arises. Existing methods are heavily tuned for handhelds with respect to requirements for sensors, processing capability and energy supply. To allow localization on wearables devices, this work presents a distributed system approach using both, a handheld and a wearable, complementing one another. It uses a wearable of low complexity, resembling currently available and affordable fitness trackers.

In a *standalone mode* only handhelds are used for loalization. Once the user leaves the handheld behind on a furniture, the *joint mode* becomes active, localizing the the user relative to the handheld using a common Bluetooth LE connection. For it, a dead-reckoning approach in combinations with distance-based calibration is used. A particle filter fuses information from these two sources. In addition a handoff mechanic has been implemented where the wearable will not expend energy, when it is close to the handheld. The system achieves a localization accuracy of 90.3% for a trial of 10 subjects. Handoff reliability was found to be as high as 97%.

The system presents a promising notion for wearable localization in the future. Before that however, practical limitations originating from wave propagation phenomena as well as wearable positioning on the body have to be solved to allow truly non-intrusive and thus pervasive indoor localization.

Bibliography

[1] E. Workgroup, "Buildings and their impact on the environment: a statistical summary," tech. rep., Technical Report, US Environmental Protection Agency, 2009.

[2] A. Hopper, A. Harter, and T. Blackie, "The active badge system," in *Proceedings of the INTERACT'93 and CHI'93 Conference on Human Factors in Computing Systems*, pp. 533–534, ACM, 1993.

[3] D. Lymberopoulos, J. Liu, X. Yang, R. R. Choudhury, V. Handziski, and S. Sen, "A realistic evaluation and comparison of indoor location technologies: Experiences and lessons learned," in *Proceedings of the 14th international conference on information processing in sensor networks*, pp. 178–189, ACM, 2015.

[4] A. Török, A. Nagy, L. Kováts, and P. Pach, "Drear-towards infrastructure-free indoor localization via dead-reckoning enhanced with activity recognition," in *2014 Eighth International Conference on Next Generation Mobile Apps, Services and Technologies*, pp. 106–111, IEEE, 2014.

[5] W. Kang and Y. Han, "Smartpdr: Smartphone-based pedestrian dead reckoning for indoor localization," *IEEE Sensors journal*, vol. 15, no. 5, pp. 2906–2916, 2015.

[6] S. Kumar, S. Gil, D. Katabi, and D. Rus, "Accurate indoor localization with zero start-up cost," in *Proceedings of the 20th annual international conference on Mobile computing and networking*, pp. 483–494, ACM, 2014.

[7] V. Woods and R. Van der Meulen, "Gartner says worldwide wearable devices sales to grow 18.4 percent in 2016," 2016. Available: `http://gartner.com/` [Accessed Sep. 23, 2016].

[8] C. Sarkar, A. Uttama Nambi SN, and R. Venkatesha Prasad, "iltc: Achieving individual comfort in shared spaces," in *Proceedings of the International Conference on Embedded Wireless Systems and Networks (EWSN)*, ACM, 2016.

[9] M. A. Stelios, A. D. Nick, M. T. Effie, K. M. Dimitris, and S. C. Thomopoulos, "An indoor localization platform for ambient assisted living using uwb," in *Proceedings of the 6th international conference on advances in mobile computing and multimedia*, pp. 178–182, ACM, 2008.

[10] S. Kozina, H. Gjoreski, M. Gams, and M. Luštrek, "Efficient activity recognition and fall detection using accelerometers," in *International Competition on Evaluating AAL Systems through Competitive Benchmarking*, pp. 13–23, Springer, 2013.

[11] K. Myers, P. Berry, J. Blythe, K. Conley, M. Gervasio, D. L. McGuinness, D. Morley, A. Pfeffer, M. Pollack, and M. Tambe, "An intelligent personal assistant for task and time management," *AI Magazine*, vol. 28, no. 2, p. 47, 2007.

[12] M. Gibney, "Product chart," 2016. Available: `http://productchart.com/` [Accessed Sep. 23, 2016].

[13] V. Woods and R. Van der Meulen, "Apple watch battery size half as big as top android wear watch," 2015. Available: `http://techradar.com/` [Accessed Sep. 23, 2016].

[14] F. Hong, Y. Zhang, Z. Zhang, M. Wei, Y. Feng, and Z. Guo, "Wap: Indoor localization and tracking using wifi-assisted particle filter," in *39th Annual IEEE Conference on Local Computer Networks*, pp. 210–217, IEEE, 2014.

[15] Z. Xiao, H. Wen, A. Markham, and N. Trigoni, "Lightweight map matching for indoor localisation using conditional random fields," in *Information Processing in Sensor Networks, IPSN-14 Proceedings of the 13th International Symposium on*, pp. 131–142, IEEE, 2014.

[16] H. Wang, S. Sen, A. Elgohary, M. Farid, M. Youssef, and R. R. Choudhury, "No need to war-drive: unsupervised indoor localization," in *Proceedings of the 10th international conference on Mobile systems, applications, and services*, pp. 197–210, ACM, 2012.

[17] A. Rai, K. K. Chintalapudi, V. N. Padmanabhan, and R. Sen, "Zee: zero-effort crowdsourcing for indoor localization," in *Proceedings of the 18th annual international conference on Mobile computing and networking*, pp. 293–304, ACM, 2012.

[18] R. Bajaj, S. L. Ranaweera, and D. P. Agrawal, "Gps: location-tracking technology," *Computer*, vol. 35, no. 4, pp. 92–94, 2002.

[19] G. Ding, J. Zhang, Z. Tan, *et al.*, "Overview of received signal strength based fingerprinting localization in indoor wireless lan environments," in *Microwave, Antenna, Propagation and EMC Technologies for Wireless Communications (MAPE), 2013 IEEE 5th International Symposium on*, pp. 160–164, IEEE, 2013.

[20] L. Calderoni, M. Ferrara, A. Franco, and D. Maio, "Indoor localization in a hospital environment using random forest classifiers," *Expert Systems with Applications*, vol. 42, no. 1, pp. 125–134, 2015.

[21] M. D. Redžić, C. Brennan, and N. E. O'Connor, "Seamloc: Seamless indoor localization based on reduced number of calibration points," *IEEE Transactions on Mobile Computing*, vol. 13, no. 6, pp. 1326–1337, 2014.

[22] Y. Gao, J. Niu, R. Zhou, and G. Xing, "Zifind: Exploiting cross-technology interference signatures for energy-efficient indoor localization," in *INFOCOM, 2013 Proceedings IEEE*, pp. 2940–2948, IEEE, 2013.

[23] C. Wu, Z. Yang, Y. Liu, and W. Xi, "Will: Wireless indoor localization without site survey," *IEEE Transactions on Parallel and Distributed Systems*, vol. 24, no. 4, pp. 839–848, 2013.

[24] J. S. Esteves, A. Carvalho, and C. Couto, "Generalized geometric triangulation algorithm for mobile robot absolute self-localization," in *Industrial Electronics, 2003. ISIE'03. 2003 IEEE International Symposium on*, vol. 1, pp. 346–351, IEEE, 2003.

[25] H. Liu, H. Darabi, P. Banerjee, and J. Liu, "Survey of wireless indoor positioning techniques and systems," *IEEE Transactions on Systems, Man, and Cybernetics, Part C (Applications and Reviews)*, vol. 37, no. 6, pp. 1067–1080, 2007.

[26] Y. Gu, L. Quan, F. Ren, and J. Li, "Fast indoor localization of smart hand-held devices using bluetooth," in *Mobile Ad-hoc and Sensor Networks (MSN), 2014 10th International Conference on*, pp. 186–194, IEEE, 2014.

[27] A. R. Jimenez, F. Seco, C. Prieto, and J. Guevara, "A comparison of pedestrian dead-reckoning algorithms using a low-cost mems imu," in *Intelligent Signal Processing, 2009. WISP 2009. IEEE International Symposium on*, pp. 37–42, IEEE, 2009.

[28] A. Abadleh, S. Han, S. J. Hyun, B. Lee, and M. Kim, "Ilps: Indoor localization using physical maps and smartphone sensors," in *World of Wireless, Mobile and Multimedia Networks (WoWMoM), 2014 IEEE 15th International Symposium on a*, pp. 1–6, IEEE, 2014.

[29] A. T. Mariakakis, S. Sen, J. Lee, and K.-H. Kim, "Sail: single access point-based indoor localization," in *Proceedings of the 12th annual international conference on Mobile systems, applications, and services*, pp. 315–328, ACM, 2014.

[30] S. Yang, P. Dessai, M. Verma, and M. Gerla, "Freeloc: Calibration-free crowdsourced indoor localization," in *INFOCOM, 2013 Proceedings IEEE*, pp. 2481–2489, IEEE, 2013.

[31] Z. Yang, Z. Zhou, and Y. Liu, "From rssi to csi: Indoor localization via channel response," *ACM Computing Surveys (CSUR)*, vol. 46, no. 2, p. 25, 2013.

[32] M. Hardegger, G. Tröster, and D. Roggen, "Improved actionslam for long-term indoor tracking with wearable motion sensors," in *Proceedings of the 2013 International Symposium on Wearable Computers*, pp. 1–8, ACM, 2013.

[33] M. Europe, "Mouser electronics," 2016. Available: `http://eu.mouser.com` [Accessed Sep. 23, 2016].

[34] Digi-Key, "Digi-key electronics," 2016. Available: `http://digikey.com` [Accessed Sep. 23, 2016].

[35] Samsung, "Samsung Gear Live," 2016. Available: `http://www.samsung.com/us/mobile/wearable-tech/SM-R3820ZKAXAR` [Accessed Apr. 1, 2016].

[36] Xiaomi, "Mi band," 2016. Available: `http://www.mi.com/en/miband/#03/slide2` [Accessed Apr. 1, 2016].

[37] Argenox, "A guide to selecting a bluetooth chipset," 2016. Available: `http://www.argenox.com/` [Accessed Oct. 10, 2016].

[38] A. Devices, "Adxl362," 2016. Available: `http://www.analog.com/` [Accessed Oct. 10, 2016].

[39] C. V. Bouten, K. T. Koekkoek, M. Verduin, R. Kodde, and J. D. Janssen, "A triaxial accelerometer and portable data processing unit for the assessment of daily physical activity," *IEEE Transactions on Biomedical Engineering*, vol. 44, no. 3, pp. 136–147, 1997.

[40] M. Marschollek, M. Goevercin, K.-H. Wolf, B. Song, M. Gietzelt, R. Haux, and E. Steinhagen-Thiessen, "A performance comparison of accelerometry-based step detection algorithms on a large, non-laboratory sample of healthy and mobility-impaired persons," in *2008 30th Annual International Conference of the IEEE Engineering in Medicine and Biology Society*, pp. 1319–1322, IEEE, 2008.

[41] O. Oguejiofor, V. Okorogu, A. Adewale, and B. Osuesu, "Outdoor localization system using rssi measurement of wireless sensor network," *International Journal of Innovative Technology and Exploring Engineering*, vol. 2, no. 2, pp. 1–6, 2013.

[42] J. Radatz, *The IEEE standard dictionary of electrical and electronics terms*. IEEE Standards Office, 1997.

[43] E. Elnahrawy, X. Li, and R. P. Martin, "The limits of localization using signal strength: A comparative study," in *Sensor and Ad Hoc Communications and Networks, 2004. IEEE SECON 2004. 2004 First Annual IEEE Communications Society Conference on*, pp. 406–414, IEEE, 2004.

[44] X. Huang, M. Barralet, and D. Sharma, "Accuracy of location identification with antenna polarization on rssi," in *Proceedings of the International MultiConference of Engineers and Computer Scientists*, vol. 1, Citeseer, 2009.

[45] T. S. Rappaport, "Wireless communications–principles and practice, (the book end)," *Microwave Journal*, vol. 45, no. 12, pp. 128–129, 2002.

[46] N. Roy, H. Wang, and R. Roy Choudhury, "I am a smartphone and i can tell my user's walking direction," in *Proceedings of the 12th annual international conference on Mobile systems, applications, and services*, pp. 329–342, ACM, 2014.

[47] E. M. Diaz, A. L. M. Gonzalez, and F. de Ponte Müller, "Standalone inertial pocket navigation system," in *2014 IEEE/ION Position, Location and Navigation Symposium-PLANS 2014*, pp. 241–251, IEEE, 2014.

[48] Z.-A. Deng, G. Wang, Y. Hu, and D. Wu, "Heading estimation for indoor pedestrian navigation using a smartphone in the pocket," *Sensors*, vol. 15, no. 9, pp. 21518–21536, 2015.